Advanced Composites and Hybrid Materials (2022) 5:1769–1777
https://doi.org/10.1007/s42114-022-00417-2

ORIGINAL RESEARCH

Enhanced electromagnetic wave absorption of engineered epoxy nanocomposites with the assistance of polyaniline fillers

Jiang Guo[1] · Zhuoran Chen[1] · Xiaojian Xu[2] · Xu Li[1] · Hu Liu[3] · Shaohua Xi[1] · Waras Abdul[1] · Qing Wu[1] · Pei Zhang[1] · Ben Bin Xu[4] · Jianfeng Zhu[1] · Zhanhu Guo[5]

Received: 1 November 2021 / Revised: 15 December 2021 / Accepted: 2 January 2022 / Published online: 12 January 2022

Abstract

In this work, the engineered polyaniline (PANI)/epoxy composites reinforced with PANI-M (physical mixture of PANI spheres and fibers) exhibit significantly enhanced electromagnetic wave absorption performance and mechanical property. Due to the synergistic effect of PANI fillers with different geometries, the reflection loss of 10.0 wt% PANI-M/epoxy could reach − 36.8 dB at 17.7 GHz. Meanwhile, the mechanical properties (including tensile strength, toughness, and flexural strength) of PANI/epoxy were systematically studied. Compared with pure epoxy, the tensile strength of epoxy with 2.0 wt% PANI-M was improved to 86.2 MPa. Moreover, the PANI spheres (PANI-S) and PANI fibers (PANI-F) were prepared by the chemical oxidation polymerization method and interface polymerization method, respectively. The characterizations including scanning electron microscope, Fourier transform infrared spectra, and X-ray diffraction were applied to analyze the morphology and chemical and crystal structures of PANI filler. This work could provide the guideline for the preparation of advanced engineered epoxy nanocomposites for electromagnetic wave pollution treatment.

Keywords PANI/epoxy composites · Mechanical property · Synergistic effect · Electromagnetic wave absorption

1 Introduction

With the rapid rollout and extensive usage of 5G wireless communication systems and high-frequency electronic equipments, the electromagnetic wave pollution has become a serious threat to the environments and our daily life [1–5]. The electromagnetic wave interference not only affects the precision performance of sensitive electronic devices, but also human health [6–9] The electromagnetic wave absorption plays an important role in mitigating the risks induced by the electromagnetic radiation pollution [10–12]. Therefore, the development of high-performance electromagnetic wave absorption materials is of great significance to ensure the safe operation of equipment and human health.

Due to the high conductivity and good electromagnetic wave permeability, metal and magnetic materials are the traditional materials for electromagnetic wave absorption [13, 14]. However, the drawbacks of those metal and magnetic materials including poor corrosion resistance and high density restrict the practical application

✉ Jiang Guo
jguo@sust.edu.cn

✉ Ben Bin Xu
ben.xu@northumbria.ac.uk

✉ Jianfeng Zhu
zhujf@sust.edu.cn

✉ Zhanhu Guo
zguo10@utk.edu

[1] School of Materials Science and Engineering, Shaanxi Key Laboratory of Green Preparation and Functionalization for Inorganic Materials, Shaanxi University of Science & Technology, Xi'an 710021, China

[2] Gas Production Plant 3 of Petrochina Changqing Oilfield Company, Wushenqi Neimenggu 017300, China

[3] Key Laboratory of Materials Processing and Mold (Zhengzhou University), Ministry of Education, National Engineering Research Center for Advanced Polymer Processing Technology, Zhengzhou University, Zhengzhou 450001, China

[4] Mechanical and Construction Engineering, Faculty of Engineering and Environment, Northumbria University, Newcastle upon Tyne NE1 8ST, UK

[5] Integrated Composites Laboratory (ICL), Department of Chemical & Biomolecular Engineering, University of Tennessee, Knoxville, TN 37996, USA

[15, 16]. In recent years, conductive polymers and their nanocomposites have received widespread attention for electromagnetic wave absorption because of the versatility, light weight, good corrosion resistance, and adjustable electrical conduction performance [17–26]. Among them, polyaniline (PANI) shows great potential for electromagnetic wave absorption [27–30]. For instance, Zhang et al. fabricated the interwoven cellulose/PANI nanofiber composites by depositing PANI on cellulose's surface, and minimum reflection loss can reach − 49.24 dB [31]. Wang et al. reported the carbon nanotube/polyaniline composites with a reflection loss of −41.5 dB [32]. Kulkarni et al. synthesized α-MnO_2 nanorod-PANI nanocomposites using polymer coating and grafting methods. The minimum reflection loss of α-MnO_2-NH_2-PANI nanocomposites has been improved to −30.79 dB at 14.5 GHz [33]. Although PANI composites show good electromagnetic wave absorption property, the poor mechanical property of these powder composites limits their value for practical application. Hence, it is important to design the composites with electromagnetic wave absorption property and mechanical property simultaneously.

Epoxy, as an engineered thermosetting material, can be applied in different fields such as marine, aerospace, and electronic devices [34–41]. The insulated epoxy is transparent to electromagnetic wave, which can be used as matrix for electromagnetic wave absorption material. Compared with paraffin wax, epoxy shows better mechanical property and chemical resistance [41–45]. As previously reported, the minimum reflection loss of the carbon nanofiber/epoxy composites is up to 12.6 dB [46]. In our former work, we demonstrated that PANI could react with epoxy by forming the C-N covalent bond, leading to a uniform initiation of electrical conduction network in epoxy for electromagnetic wave absorption. So, the PANI/epoxy composites show great potential for electromagnetic wave absorption. Vigneras et al. reported the electromagnetic wave absorption property of epoxy nanocomposites with different morphology of PANI fillers [47]. However, the synergistic effect of different PANI fillers on the electromagnetic wave absorption and mechanical property of PANI/epoxy composites has not been reported elsewhere.

In this work, the PANI/epoxy composites with improved mechanical property and electromagnetic wave absorption property were reported. The PANI fillers with different morphologies (sphere and fiber) were prepared by the chemical oxidation polymerization (COP) method and interfacial polymerization (IP) method, respectively. The characterizations including scanning electron microscope, Fourier transform infrared spectra, and X-ray diffraction were applied to analyze the morphology and chemical and crystal structures of PANI fillers. The effects of PANI fillers on the mechanical properties (including toughness, flexural strength and tensile strength) and electromagnetic wave absorption performance are systemically studied. This work would provide the guideline for designing epoxy-based composites for electromagnetic wave pollution treatment.

2 Experimental

2.1 Materials

Monomer aniline (C_6H_7N, ≥ 99.5%), chloroform ($CHCl_3$, 99.5%), and ammonia water ($NH_3{\cdot}H_2O$, 25%) were purchased from Sinopharm Co. China. Ammonium persulfate (APS, $(NH_4)_2S_2O_9$, 98%) and *p*-toluene sulfonic acid (PTSA, $C_7H_8O_3SH_2O$, 98.5%) were obtained from Tianjin Kermel, China. Ethanol was supplied by Fuyu Fine Chemical Co. China. The epoxy resin (Epon 862, ≥ 99.8% with epoxy value: 5.8 − 6.1 mol/kg, density: 1.18 g/cm^{-3}) was purchased from Guangzhou Picks Chemical Co. China. Diethyl methyl benzene diamine (DETDA, $C_{11}H_{18}N_2$, ≥ 98%) as curing agent was bought from Jining Baichuan Chemical Co. China. Scheme 1 exhibits the molecular structures of Epon 862 and DETDA.

2.2 Synthesis of PANI fillers

The PANI fiber (PANI-F) was prepared through the interfacial polymerization method at room temperature. The molar ratio of aniline/APS/PTSA was 8:2:25. Firstly, 8 mmol APS was added into 100 ml PTSA aqueous solution (1 mol/L) as solution 1, and 32 mmol aniline solution dissolved in 100 ml

Scheme 1 Molecular structure of Epon 862 and DETDA

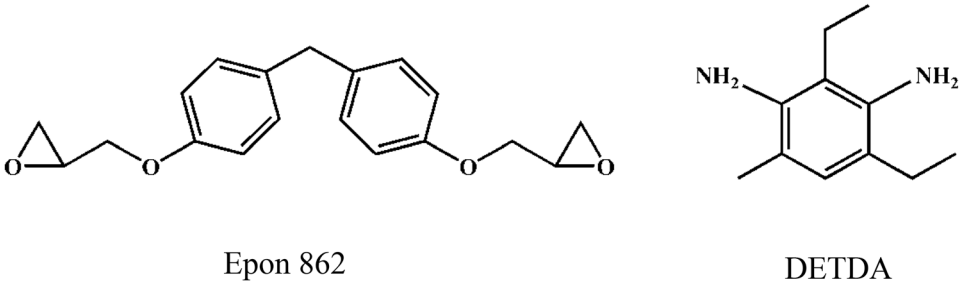

Epon 862 DETDA

chloroform as solution 2. Second, solution 1 was rapidly added into solution 2 and remained there for 2 h for polymerization of aniline monomers. Then, the product was treated by vacuum filtration and washed with ethanol and deionized water several times to remove organic solvent, oligomers, and additional acid. After that, the obtained final products were dried in the oven at 50 °C for 12 h.

The PANI sphere (PANI-S) was prepared by the COP method. For solution A, 30 mmol PTSA and 18 mmol APS were added into 200 mL deionized water and then treated by sonication and mechanical stirring for 1 h in ice-water bath. The 36 mmol aniline was added into 50 ml deionized water as solution B. Then, solution B was mixed in solution A for polymerization under mechanical and ultrasonic stirring for 2 h in an ice-water bath. The product was treated by vacuum filtration, washed with ethanol and water several times, and dried at 50 °C. To make the same amount of proton acid doping level for PANI fillers, the obtained PANI-S was soaked in ammonia water (1 mol/L) for 10 min, then washed several times with water and dried at 50 °C. After that, the product was soaked in PTSA solution (1 mol/L) for 10 min and washed several times with water to remove acid. The final obtained samples were dried at 50 °C for 12 h.

2.3 Fabrication of PANI/epoxy composites

Firstly, the PANI fillers were immersed in epon monomers overnight. Then, the above mixture was mechanically stirred (500 rpm) at room temperature for 1 h. After that, curing agent DETDA was added (weight ratio of epon monomer to curing agent is 100 to 26.5), then treated with mechanical stirring for additional 1 h. Then, the above suspension was mechanically stirred at 70 °C for 2 h at a speed of 200 rpm. Finally, the solutions were poured into the silicone molds and cured at 120 °C for 5 h, then cooling to ambient temperature naturally. In this work, The pure epoxy, epoxy with 10.0 wt% PANI-F, epoxy with 10.0 wt% PANI-S, and epoxy with 2.0, 6.0, and 10.0 wt% PANI mixtures (PANI-M) which includes PANI-F and PANI-S (the mass ratio of PANI-F to PANI-S was 1:1 in PANI-M) were prepared.

2.4 Characterization

FT-IR spectra were acquired on Vertex 70 using the attenuated total reflectance (resolution: 4.0 cm^{-1}). XRD of PANI fillers was recorded on D/max2200PC X-ray diffractometer with Cu Kα radiation ($\lambda = 1.5418$ Å; scan rate: 6°min^{-1}). SEM was carried out using a FEI Verios 460 microscope to observe the morphology of the fabricated PANI samples and the fractured surfaces of PANI/epoxy nanocomposites. Mechanical properties of pure epoxy and epoxy nanocomposites were measured at least 3 times at room temperature including tensile test and bending performance test. Tensile measurements were carried out using the AI-7000GD unidirectional tensile testing machine (crosshead speed: 1.00 mm/min). The samples were bone-like according to ASTM (D412-98a, 2002) requirement. Bending measurements were characterized at a speed of 0.50 mm/min by strength in three-point bending using the 1036PC unidirectional tensile testing machine. The sample dimensions were $60 \times 12 \times 3$ mm, which were designed according to the GB/T requirement. Dielectric properties and volume resistivity of the samples were conducted by Agilent E4980AL in the range of 5×10^3 to 1×10^6 Hz at room temperature. The reflection loss of epoxy nanocomposites was obtained through a vector network analyzer, E5071C, Agilent Technology, in the frequency range of 2–18 GHz under air condition at room temperature. The sample was shaped as a ring, with the inner and outer diameter of 3.04 and 7.00 mm, respectively.

3 Results and discussion

3.1 Characterizations for PANI fillers

Figure 1A and B exhibit SEM images of different PANI-F and PANI-S prepared by two different methods. The average diameter of PANI-F and PANI-S is 105 and 170 nm measured by nanomeasurer software, respectively. The rough surface of PANI-S is due to the insufficient time for aniline monomer to grow along the molecular chain under sonication treatment and mechanical stirring. For the FT-IR of PANI-F and PANI-S in Fig. 1C, the characteristic peaks at 1558 and 1488 cm^{-1} are attributed to C = C stretching of the quinoid rings and bezenoid rings [28, 48]. The peak at 1295 cm^{-1} is assigned to the C–N stretching vibration of the secondary amine [49], indicating the conducting emeraldine salt form of PANI originating from the bipolaron structure [50]. The peak 1240 cm^{-1} is related to the C–N stretching vibration of the polaronic structure. The peak at 796 cm^{-1} is attributed the C–H out-of-plane bending vibrations of the benzenoid ring [51]. The peaks located at 1240 and 1124 cm^{-1} are assigned to C–H bendings of the benzenoid ring and the quinonoid ring, respectively [52]. The XRD diffraction is shown in Fig. 1D. There are three diffraction peaks at around 14.8°, 19.8°, and 25.4° correspond to the (010), (100), and (110) crystallographic planes of the partially crystallized PANI nanostructure [53]. All the above results confirm that PANI-F and FANI-S were successfully synthesized by two different methods

3.2 Mechanical property

Figure 2 demonstrates the stress–strain curves of epoxy nanocomposites with various PANI fillers. The tensile strength of

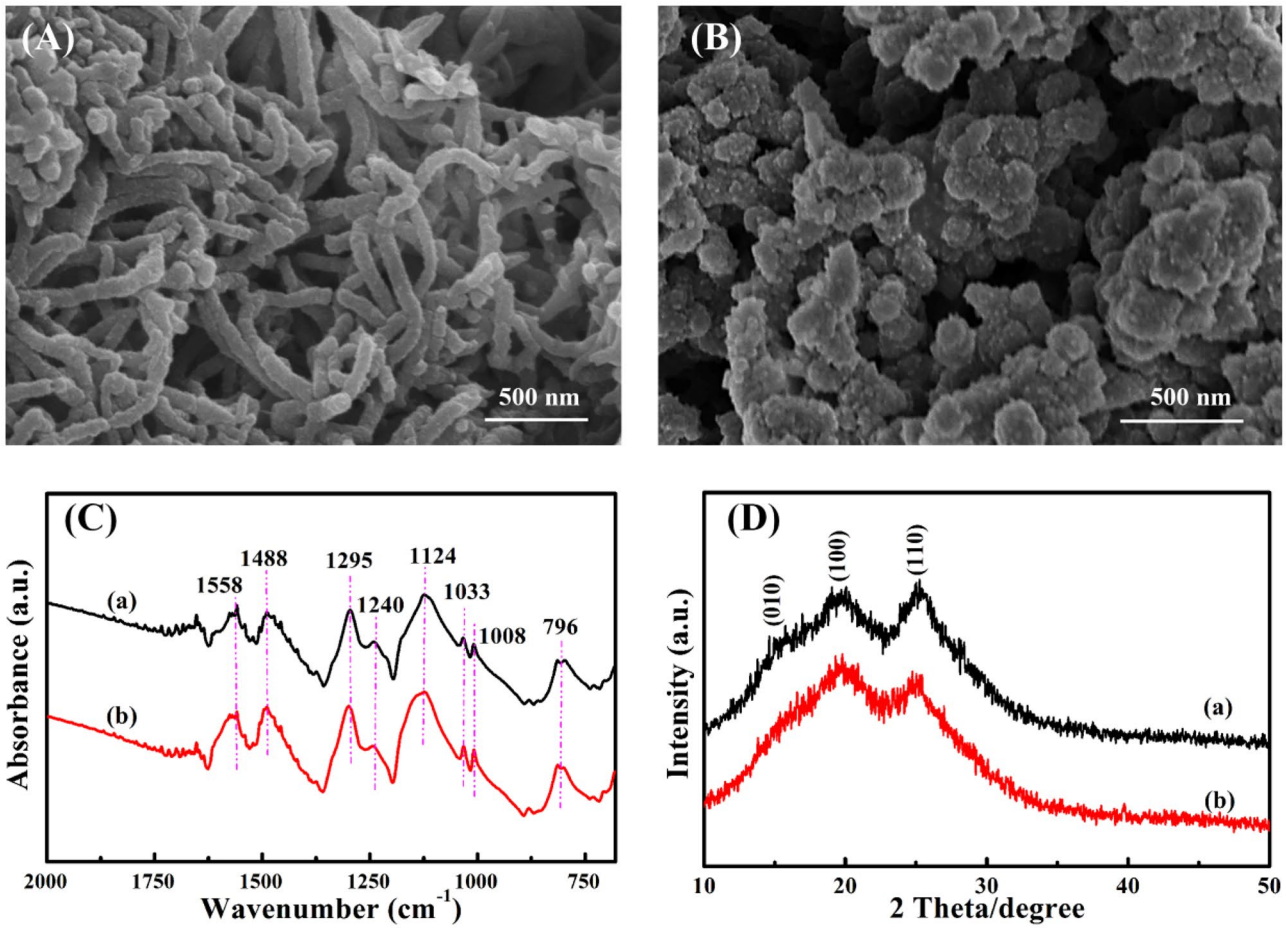

Fig. 1 SEM images of **A** PANI-F and **B** PANI-S, **C** FT-IR spectra and **D** XRD patterns of a PANI-F and b PANI-S

epoxy with 2.0 wt% PANI-M is 86.2 MPa, which is larger than tensile strength (84.9 MPa) of pure epoxy. Compared with 2.0 wt% PANI-M/epoxy, the tensile strength of 6.0 wt% PANI-M/epoxy and 10.0 wt% PANI-M/epoxy is much lower (69.7 and 61.3 MPa), which is due to the agglomeration of PANI filler in epoxy, and the similar result is observed in polypyrrole/epoxy nanocomposites as well [54]. When the loading of the PANI filler is 10.0 wt%, the tensile strength (82.1 MPa) of PANI-F/epoxy is larger than that of epoxy with PANI-S (65.1 MPa) and PANI-M (61.3 MPa). The epoxy nanocomposites with different PANI fillers show larger Young's modulus than pure epoxy, indicating stiff interfacial layer formed between PANI and epoxy [55]. Flexural strength indicates the tendency for a material to resist bending in flexural deformation. Compared with pure epoxy (137.9 MPa), the flexural strength of PANI-M/epoxy nanocomposites is lower and decreases with the increase of PANI-M loading. The flexural strength (97.7 MPa) of 10.0% PANI-F/epoxy is larger than that of epoxy with PANI-S (62.5 MPa) and PANI-M (72.9 MPa). The toughness for all the samples shows the same tendency as the flexural strength. The Young's modulus, flexural strength, and toughness are summarized in Table 1. The PANI filler could reduce the flexural strength and toughness of epoxy, but enhance its Young's modulus, demonstrating that stiffness is enhanced by sacrificing the flexural strength and toughness. It is worth noticing that the PANI-F/epoxy nanocomposites show larger tensile strength, flexural strength and toughness than epoxy with PANI-S and PANI-M fillers when the loading level of PANI fillers is same.

SEM image of the fracture surface after tensile test is applied to study the effect of PANI fillers on tensile strength (Fig. 3). The pure epoxy displays a relatively smooth fracture surface with "river-like" pattern, indicating a typical brittle fracture because of rapid propagation of the cracks [56] (Fig. 3a). However, compared with pure epoxy, the fracture surface of epoxy nanocomposites reinforced with PANI fillers become much rougher. For 2.0 wt% PANI-M/epoxy, the PANI fillers are well dispersed in the epoxy matrix (Fig. 3b), and the "river-like" pattern disappeared which indicates the strong covalent bond between PANI and epoxy matrix [57]. This formed covalent bond cannot only enhance the compatibility, but also enhance interfacial adhesion between the two

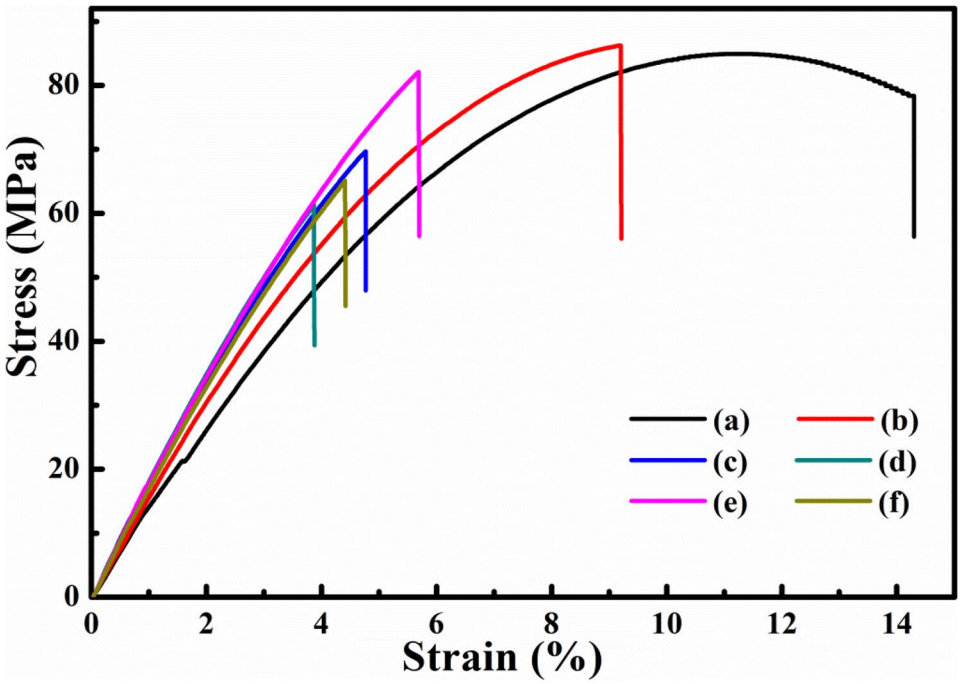

Fig. 2 Stress–strain curves for a pure epoxy and PANI/epoxy nanocomposites with b 2.0 wt% PANI-M, c 6.0 wt% PANI-M, d 10.0 wt% PANI-M, e 10.0 wt% PANI-F and f 10.0 wt% PANI-S

phases [58]. Therefore, the tensile strength of 2.0 wt% PANI-M/epoxy is larger than that of pure epoxy. With increasing the PANI filler loading (Fig. 3c–f), the agglomeration of PANI fillers are observed in the epoxy nanocomposites, which lead to the deceasing of tensile strength. When the PANI loading is 10.0 wt%, it is observed that the PANI-F/epoxy show much rougher fracture surface than epoxy with PANI-M or PANI-S, indicating PANI-F makes more contribution to obstruct the propagation of the cracks [26]. Thus, the PANI-F/epoxy nanocomposites show higher tensile strength when the PANI nanofiller loading is 10.0 wt%.

3.3 Electromagnetic wave absorption performance

In general, the real parts (ε′ and μ′) and imaginary parts (ε″ and μ") represent the storage and loss of electrical and magnetic energy, respectively. The values of electromagnetic parameters (ε′, ε″, μ′, and μ") of PANI/epoxy nanocomposites are shown in Fig. 4. The positive dielectric constant of PANI/epoxy composites is due to interfacial polarization formed at the interface between PANI fillers and epoxy matrix. The charge carriers were hindered by the epoxy resin, resulting in the accumulation of space charge carriers at the interface between PANI fillers and epoxy matrix [59]. In Fig. 4a–c, the ε′ increases with increasing PANI-M content at the same frequency. For PANI/epoxy composites with 10.0 wt% PANI fillers, Fig. 4c–e, it is obvious to observe that the ε′ increase with increasing PANI-F content, which is due to the larger specific surface area of PANI-F. And ε″ exhibits the same variation pattern as ε′. The μ′ and μ″ of the PANI/epoxy is about 1 and 0, demonstrating magnetic loss does not make contribution to convert the electromagnetic wave energy to heat.

Generally, the electromagnetic wave absorption property of a material is related to the complex permittivity and permeability [60]. The reflection loss (RL) can be expressed as Eq. 1 [61]:

$$RL = 20\log\frac{|Z_{in} - Z_0|}{|Z_{in} + Z_0|} \quad (1)$$

Table 1 Young's modulus, flexural strength, and toughness of pure epoxy and PANI/epoxy nanocomposites with different PANI nanofillers

	Pure Epoxy	2.0 wt% PANI-M	6.0 wt% PANI-M	10.0 wt% PANI-M	10.0 wt% PANI-F	10.0 wt% PANI-S
Young's modulus (GPa)	1.4	1.6	1.8	1.8	1.8	1.7
Flexural strength (MPa)	137.9	106.0	104.0	72.9	97.7	62.5
Toughness (J m^{-3} 10^4)	885.4	506.2	181.6	127.0	258.9	154.0

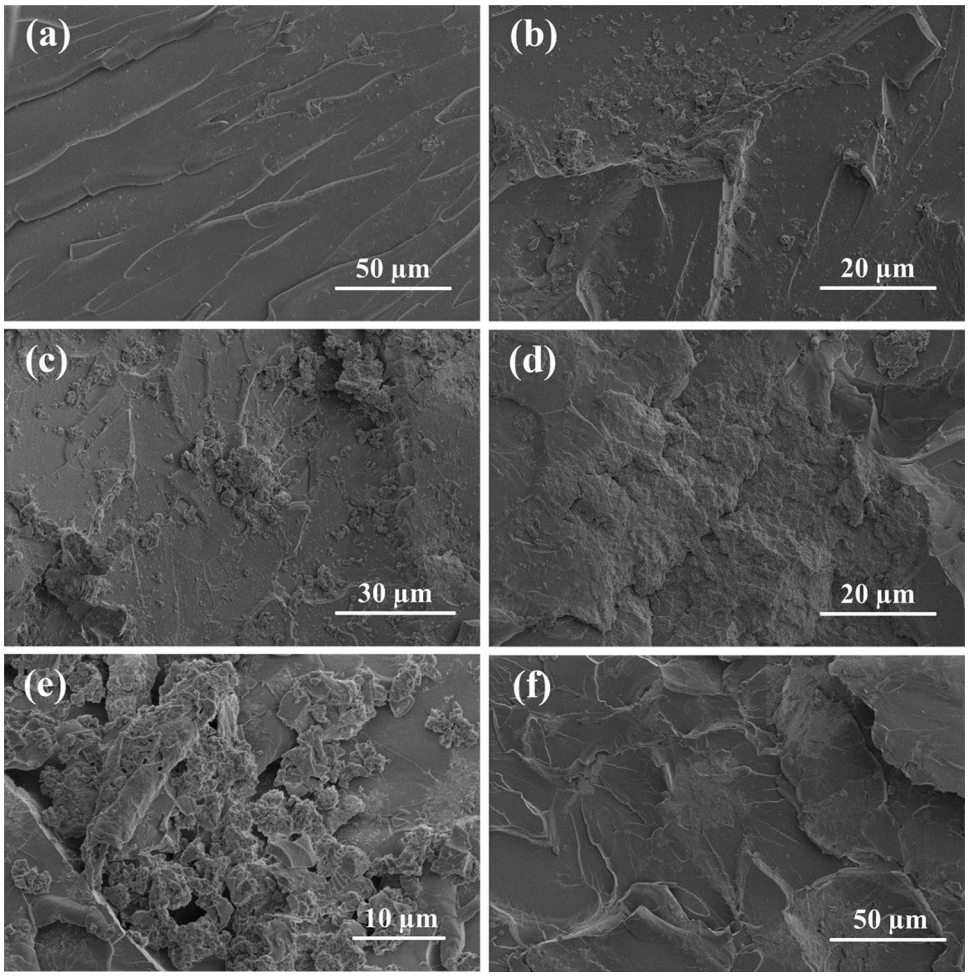

Fig. 3 SEM images of the fracture surface after tensile test of **a** cured pure epoxy and PANI/epoxy nanocomposites with **b** 2.0 wt% PANI-M, **c** 6.0 wt% PANI-M, **d** 10.0 wt% PANI-M, **e** 10.0 wt% PANI-F and **f** 10.0 wt% PANI-S

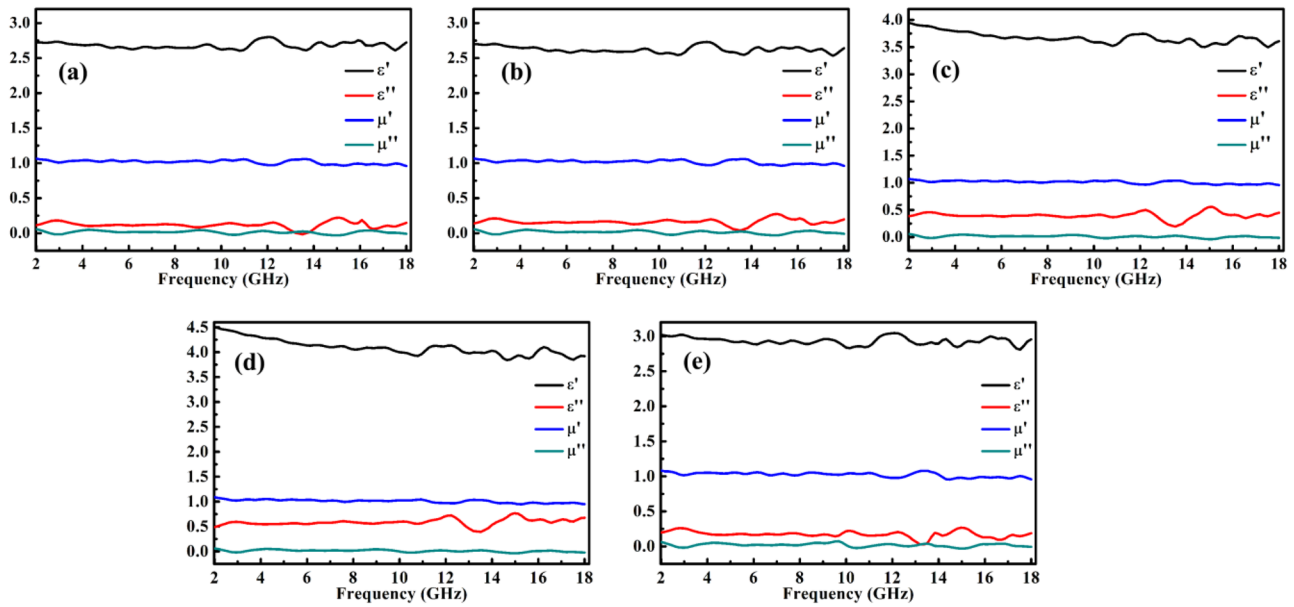

Fig.4 Permittivity and permeability as a function of frequency for PANI/epoxy nanocomposites with **a** 2.0 wt% PANI-M, **b** 6.0 wt% PANI-M, **c** 10.0 wt% PANI-M, **d** 10.0 wt% PANI-F and **e** 10.0 wt% PANI-S

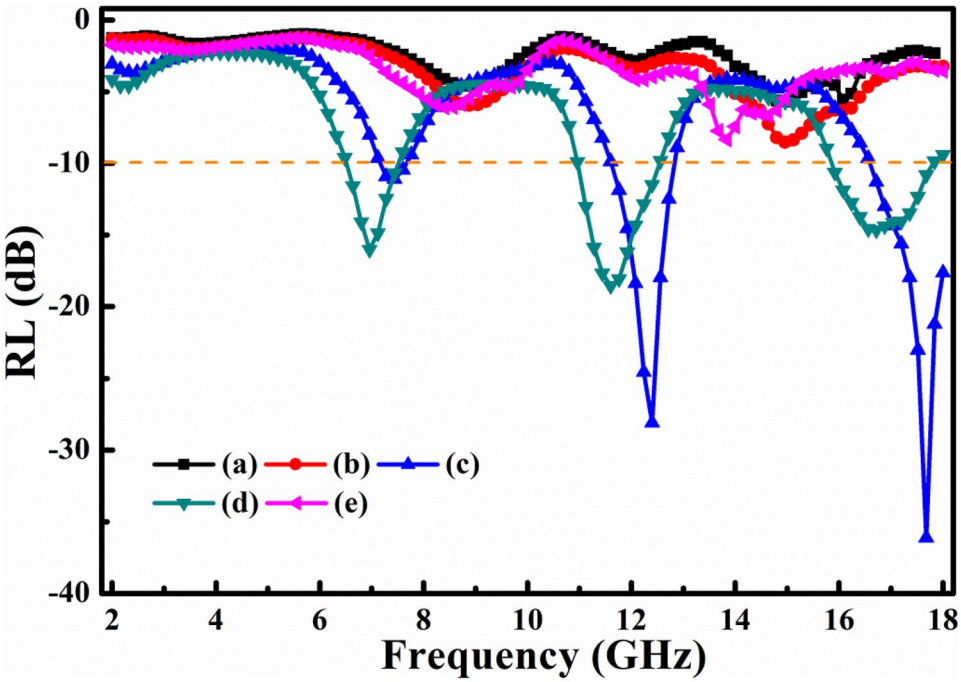

Fig. 5 RL as a function of frequency for PANI/epoxy nanocomposites with a 2.0 wt% PANI-M b 6.0 wt% PANI-M c 10.0 wt% PANI-M, d 10.0 wt% PANI-F and e 10.0 wt% PANI-S

where Z_{in} is the effective input impedance, and Z_0 is the impedance in free space. Z_{in} is given by Eq. 2 [62]:

$$Z_{in} = Z_0\sqrt{\mu_r/\varepsilon_r}\tanh(j\frac{2\pi fd}{c}\sqrt{\mu_r\varepsilon_r}) \quad (2)$$

where c, f, and d stand for light velocity, frequency of electromagnetic wave, and thickness of the absorber, respectively. The RL of with PANI-S/epoxy, PANI-F/epoxy, and PANI-M/epoxy is shown in Fig. 5.

Figure 5 exhibits the RL of PANI/epoxy with different PANI fillers. It can be seen that the 10.0 wt% PANI-M/epoxy nanocomposites achieve a minimum RL value of −36.8 dB at 17.7 GHz, and the bandwidth (RL below – 10 dB) is 0.3 (7.5–7.8 GHz), 1.5 (11–12.5 GHz), and 1.5 GHz (16.5–18 GHz). The 10.0 wt% PANI-F/epoxy nanocomposites achieves a minimum RL of −19.8 dB at 11.6 GHz and a bandwidth (RL below −10 dB) is 0.5 (7.0–7.5 GHz), 0.9 (10.1–12 GHz), and 1.5 GHz (16–17.5 GHz). However, for the 10.0 wt% PANI-S/epoxy nanocomposites, the RL is larger than −10 dB from 2 to 18 GHz. For practical application, RL should be less than –10 dB at least. Generally, a good impedance matching is the prerequisite for good electromagnetic wave absorption materials, and a larger difference between permittivity and permeability would lead to a worse impedance matching [59]. In this work, with increasing PANI-M loading, the difference between them is larger in the PANI-M/epoxy. So, the 10 wt% PANI-M/epoxy shows worse impedance matching. On the other hand, the 10.0 wt% PANI-M/epoxy displays better dielectric loss. Hence, the 10.0 wt% PANI-M/epoxy shows better electromagnetic wave absorption performance than epoxy with lower loading of PANI-M. When the PANI filler's loading is 10.0 wt%, although PANI-M/epoxy shows worse impedance matching than PANI-S/epoxy, the PANI-M/epoxy still exhibits better electromagnetic wave absorption performance which may be due to the synergistic effect of PANI-F and PANI-S on the interfacial polarization and dielectric loss. The similar phenomenon is observed in polyvinylpyrrolidone@multi-walled carbon nanotubes/graphene composites for electromagnetic wave absorption [63].

4 Conclusion

In this study, epoxy resin was used as the matrix, and PANI with different morphologies was used as the reinforcing material. The tensile strength of epoxy with 2.0 wt% PANI-M can reach 86.2 MPa. Moreover, a hard interface layer is formed between PANI and epoxy matrix, which improves the Young's modulus of the PANI/epoxy. The minimum RL of 10.0 wt% PANI-M/epoxy nanocomposites reach −36.8 dB, due to the synergistic effect of the mixed PANI fillers (PANI-F and PANI-S). We hope the described PANI/epoxy nanocomposites lay foundation for future engineering applications that need both good electromagnetic wave absorption performance and mechanical property.

Supplementary Information The online version contains supplementary material available at https://doi.org/10.1007/s42114-022-00417-2.

Funding The work is supported by the Research Starting Foundation of Shaanxi University of Science and Technology (Grant No.

2019QNBJ-01), the Research Foundation for Thousand Young Talent Plan of Shaanxi province of China, and the National Natural Science Foundation of China (Grant No. 51972200 and Grant No. 51902192).

Declarations

Conflict of interest The authors declare no competing interests.

References

1. Xie Q, Yan Z, Qin F, Wang L, Mei L, Zhang Y, Wang Z, Zhao G, Jiang R (2020) Metal carbide/Ni hybrids for high-performance electromagnetic absorption and absorption-based electromagnetic interference shielding. Inorg Chem Front 7:4832–4844
2. Asmatulu R, Bollavaram PK, Patlolla VR, Alarifi IM, Khan WS (2020) Investigating the effects of metallic submicron and nanofilms on fiber-reinforced composites for lightning strike protection and EMI shielding. Adv Compos Hybrid Mater 3:66–83
3. Gao Q, Pan Y, Zheng G, Liu C, Shen C, Liu X (2021) Flexible multilayered MXene/thermoplastic polyurethane films with excellent electromagnetic interference shielding, thermal conductivity, and management performances. Adv Compos Hybrid Mater 4:274–285
4. Sang G, Xu P, Yan T, Murugadoss V, Naik N, Ding Y, Guo Z-H (2021) Interface engineered microcellular magnetic conductive polyurethane nanocomposite foams for electromagnetic interference shielding. Nanomicro Lett 13:153
5. Guo J, Li X, Chen ZR, Zhu J-F, Mai X, Wei R, Sun K, Liu H, Chen Y, Naik N, Guo Z-H (2022) Magnetic $NiFe_2O_4$/polypyrrole nanocomposites with enhanced electromagnetic wave absorption. J Mater Sci Technol 108:64–72
6. Qin F, Yan Z, Fan J, Cai J, Zhu X, Zhang X (2020) Highly uniform and stable transparent electromagnetic interference shielding film based on silver nanowire–PEDOT:PSS composite for high power microwave shielding. Macromol Mater Eng 306:2000607
7. Siriwitpreecha A, Rattanadecho P, Wessapan T (2013) The influence of wave propagation mode on specific absorption rate and heat transfer in human body exposed to electromagnetic wave. Int J Heat Mass Transf 65:423–434
8. Thomassin JM, Jerome C, Pardoen T, Bailly C, Huynen I, Detrembleur C (2013) Polymer/carbon based composites as electromagnetic interference (EMI) shielding materials. Mater Sci Eng R Rep 74:211–232
9. Wang Y, Wang P, Du Z, Liu C, Shen C, Wang Y (2021) Electromagnetic interference shielding enhancement of poly(lactic acid)-based carbonaceous nanocomposites by poly(ethylene oxide)-assisted segregated structure: a comparative study of carbon nanotubes and graphene nanoplatelets. Adv Compos Hybrid Mater 1–11
10. Faisal MF, Khasim S (2014) Ku-band EMI shielding effectiveness and dielectric properties of Polyaniline-Y_2O_3 composites. Polym Sci Ser A 56:366–372
11. Cheng H, Pan Y, Chen Q, Che R, Zheng G, Liu C, Shen C, Liu X (2021) Ultrathin flexible poly(vinylidene fluoride)/MXene/silver nanowire film with outstanding specific EMI shielding and high heat dissipation. Adv Compos Hybrid Mater 4:505–513
12. Wu N, Qiao J, Liu J, Du W, Xu D, Liu W (2021) Strengthened electromagnetic absorption performance derived from synergistic effect of carbon nanotube hybrid with Co@C beads. Adv Compos Hybrid Mater 1:149–159
13. Engin FZ, Usta I (2014) Development and characterisation of polyaniline/polyamide (PANI/PA) fabrics for electromagnetic shielding. J Text Inst 106:872–879
14. Li Y, Qing Y, Li W, Zong M, Luo F (2021) Novel Magnéli Ti_4O_7/Ni/poly(vinylidene fluoride) hybrids for high-performance electromagnetic wave absorption. Adv Compos Hybrid Mater 1–12
15. Sankaran S, Deshmukh K, Ahamed MB, Khadheer PSK (2018) Recent advances in electromagnetic interference shielding properties of metal and carbon filler reinforced flexible polymer composites: a review. Compos Part A: Appl Sci Manuf 114:49–71
16. Wu N, Zhao B, Liu J, Li Y, Chen Y, Chen L, Wang M, Guo Z-H (2021) MOF-derived porous hollow Ni/C composites with optimized impedance matching as lightweight microwave absorption materials. Adv Compos Hybrid Mater 4:707–715
17. Zhu Q, Huang Y, Li Y, Zhou M, Xu S, Liu X, Liu C, Yuan B, Guo Z-H (2021) Aluminum dihydric tripolyphosphate/polypyrrole-functionalized graphene oxide waterborne epoxy composite coatings for impermeability and corrosion protection performance of metals. Adv Compos Hybrid Mater 4:780–792
18. Guo J, Xu L, Liu H, Young D, Song G, Song K, Zhu J-F, Kong J, Guo Z-H (2021) Tunable magnetoresistance of core-shell structured polyaniline nanocomposites with 0-, 1-, and 2-dimensional nanocarbons. Adv Compos Hybrid Mater 4:51–64
19. Lyu L, Liu J, Liu H, Liu C, Lu Y, Sun K, Fan R, Wang N, Lu N, Guo Z-H, Wujcik EK (2018) An overview of electrically conductive polymer nanocomposites toward electromagnetic interference shielding. Eng Sci 2(47):26–42
20. Kashfipour MA, Mehra N, Zhu J (2018) A review on the role of interface in mechanical, thermal, and electrical properties of polymer composites. Adv Compos Hybrid Mater 1:415–439
21. Luo X, Yang G, Schubert DW (2021) Electrically conductive polymer composite containing hybrid graphene nanoplatelets and carbon nanotubes: synergistic effect and tunable conductivity anisotropy. Adv Compos Hybrid Mater 1–13
22. Hu Q, Zhou J, Qiu B, Wang Q, Song G, Guo Z-H (2021) Synergistically improved methane production from anaerobic wastewater treatment by iron/polyaniline composite. Adv Compos Hybrid Mater 4:265–273
23. Gao C, Gu H, Du A, Zhou H, Pan D, Naik N, Guo Z-H (2021) Polyaniline facilitated curing of phthalonitrile resin with enhanced processibility and mechanical property. Polymer 219: 123533
24. Ingle RV, Shaikh SF, Bhujbal PK, Pathan HM, Tabhane VA (2020) Polyaniline doped with protonic acids: optical and morphological studies. ES Mater Manuf 8:54–59
25. Xu X, Fu Q, Gu H, Guo Y, Zhou H, Zhang J, Pan D, Wu S, Dong M, Guo Z-H (2020) Polyaniline crystalline nanostructures dependent negative permittivity metamaterials. Polymer 188: 122129
26. Gu H, Xu X, Cai J, Wei S, Wei H, Liu H, Young DP, Shao Q, Wu S, Ding T, Guo Z-H (2019) Controllable organic magnetoresistance in polyaniline coated poly(p-phenylene-26-benzobisoxazole) short fibers. Chem Commun 55:10068–10071
27. Li S, Yang C, Sarwar S, Nautiyal A, Zhang P, Du H, Liu N, Yin J, Deng K, Zhang X (2019) Facile synthesis of nanostructured polyaniline in ionic liquids for high solubility and enhanced electrochemical properties. Adv Compos Hybrid Mater 2:279–288
28. Guo J, Chen Z-R, Abdul W, Kong J, Khan M, David Y, Zhu J-F, Guo Z-H (2021) Tunable positive magnetoresistance of

magnetic polyaniline nanocomposites. Adv Compos Hybrid Mater 4:534–542
29. Ma Y, Zhuang Z, Ma M, Yang Y, Li W, lin J, Dong M, Wu S, Ding T, Guo Z-H (2019) Solid polyaniline dendrites consisting of high aspect ratio branches self-assembled using sodium lauryl sulfonate as soft templates: synthesis and electrochemical performance. Polymer 182:121808
30. Zhuang Z, Wang W, Wei Y, Li T, Ma M, Ma Y (2021) Preparation of polyaniline nanorods/manganese dioxide nanoflowers core/shell nanostructure and investigation of electrochemical performances. Adv Compos Hybrid Mater 4:938–945
31. Zhang Z, Wang G, Gu W, Zhao Y, Tang S, Ji G (2021) A breathable and flexible fiber cloth based on cellulose/polyaniline cellular membrane for microwave shielding and absorbing applications. J Colloid Interface Sci 605:193–203
32. Wang Y, Sun W, Lin H, Gao P, Gao J, Dai K, Yan D, Li Z (2020) Steric stabilizer-based promotion of uniform polyaniline shell for enhanced electromagnetic wave absorption of carbon nanotube/polyaniline hybrids. Compos Part B: Eng 199:108309
33. Kulkarni GK, Jadhav SA, Patil KT, Patil PS, Puri VR (2021) α-MnO_2 nanorods-polyaniline (PANI) nanocomposites synthesized by polymer coating and grafting approaches for screening EMI pollution. Ceram Int 47:15044–15051
34. Gu H, Zhang H, Ma C, Xu X, Wang Y, Wang Z, Wei R, Liu H, Liu C, Shao Q, Mai X, Guo Z-H (2019) Trace electrosprayed nanopolystyrene facilitated dispersion of multiwalled carbon nanotubes: Simultaneously strengthening and toughening epoxy. Carbon 142:131–140
35. Zhang Y, Zhan L (2020) Preparation and Damping Properties of Al_2O_3 Hollow Spheres/Epoxy Composites Encapsulating Q195 Steel Pipes. ES Mater Manuf 10:60–66
36. Jing X, Wei J, Liu Y, Song B, Liu Y (2020) Deployment analysis of aramid fiber reinforced shape-memory epoxy resin composites. Eng Sci 11:44–53
37. Chen F, Xiao H, Peng ZQ, Zhang ZP, Rong MZ, Zhang MQ (2021) Thermally conductive glass fiber reinforced epoxy composites with intrinsic self-healing capability. Adv Compos Hybrid Mater 4:1048–1058
38. Shi K, Shen Y, Zhang Y, Wang T (2018) A modified imidazole as a novel latent curing agent with toughening effect for epoxy. Eng Sci 5(2):66–72
39. Sabu M, Bementa E, Jaya Vinse Ruban Y, Ginil Mon S (2020) A novel analysis of the dielectric properties of hybrid epoxy composites. Adv Compos Hybrid Mater 3:325–335
40. Madhusudhana AM, Mohana KNS, Hegde MB, Nayak SR, Rajitha K, Swamy NK (2020) Functionalized graphene oxide-epoxy phenolic novolac nanocomposite: an efficient anticorrosion coating on mild steel in saline medium. Adv Compos Hybrid Mater 3:141–155
41. Li J, Zhang P, He H, Zhai S, Xian Y, Ma W, Wang L (2019) Enhanced thermal transport properties of epoxy resin thermal interface materials. ES energy environ 4(6):41–47
42. Wu Q, Zhao R, Zhu J, Wang F (2020) Interfacial improvement of carbon fiber reinforced epoxy composites by tuning the content of curing agent in sizing agent. Appl Surf Sci 504: 144384
43. Adak NC, Chhetri S, Murmu NC, Samanta P, Kuila T (2019) Analytical and experimental investigation on magnetorheological behavior of $CoFe_2O_4$-rGO-incorporated epoxy fluid composites. Adv Compos Hybrid Mater 2:266–278
44. Mohan PR (2013) A critical review: the modification, properties, and applications of epoxy resins. Polym Plast Technol Eng 52:107–125
45. Xia H, Li J, Wang K, Hou X, Yang T, Hu J, Shi Z (2021) Superior wear resistance of epoxy composite with highly dispersed graphene spheres. Adv Compos Hybrid Mater. https://doi.org/10.1007/s42114-021-00259-4
46. Chakradhary VK, Juneja S, Jaleel Akhtar M (2020) Correlation between EMI shielding and reflection loss mechanism for carbon nanofiber/epoxy nanocomposite. Mater Today Commun 25:101386
47. Oyharçabal M, Olinga T, Foulc MP, Lacomme S, Gontier E, Vigneras V (2013) Influence of the morphology of polyaniline on the microwave absorption properties of epoxy polyaniline composites. Compos Sci Technol 74:107–112
48. Cai J, Wang W, Pan D, Young DP, Gu H, Guo Z-H (2020) Electrical transport in polyaniline–barium ferrite nanocomposites with negative giant magnetoresistance. J Phys Chem C 124:22646–22655
49. Yao F, Xie W, Yang M, Zhang H, Gu H, Du A, Naik N, Young DP, Lin J, Guo Z-H (2021) Interfacial polymerized copolymers of aniline and phenylenediamine with tunable magnetoresistance and negative permittivity. Mater Today Phys 21:100502
50. Singh K, Ohlan A, Pham VH, RB, Varshney S, Jang JY, Hur SH, Choi WM, Kumar M, Dhawan SK, Kong BS, Chung JS, (2013) Nanostructured graphene/Fe_3O_4 incorporated polyaniline as a high performance shield against electromagnetic pollution. Nanoscale 56:2411–2420
51. Guo J, Guan L, Wei H, Khan MA, Zhang X, Li B, Wang Q, Weeks BL, Young DP, Shen T, Wei S, Guo Z-H (2016) Enhanced negative magnetoresistance with high sensitivity of polyaniline interfaced with nanotitania. J Electrochem Sci Technol 163:H664–H671
52. Cong HP, Ren XC, Wang P, Yu SH (2013) Flexible graphene–polyaniline composite paper for high-performance supercapacitor. Energy Environ Sci 6:1185–1191
53. Gu H, Wei H, Guo J, Haldolaarachige N, Young DP, Wei S, Guo Z-H (2013) Hexavalent chromium synthesized polyaniline nanostructures: magnetoresistance and electrochemical energy storage behaviors. Polymer 54:5974–5985
54. Zhang X, Yan X, Guo J, Liu Z, Jiang D, He Q, Wei H, Gu H, Colorado HA, Zhang X, Wei S, Guo Z-H (2015) Polypyrrole doped epoxy resin nanocomposites with enhanced mechanical properties and reduced flammability. J Mater Chem C 3:162–176
55. Gu H, Tadakamalla S, Zhang X, Huang Y, Jiang Y, Colorado HA, Luo Z, Wei S, Guo Z-H (2013) Epoxy resin nanosuspensions and reinforced nanocomposites from polyaniline stabilized multi-walled carbon nanotubes. J Mater Chem C 1:729–743
56. Zhang X, Alloul O, He Q, Zhu J, Verde MJ, Li Y, Wei S, Guo Z-H (2013) Strengthened magnetic epoxy nanocomposites with protruding nanoparticles on the graphene nanosheets. Polymer 54:3594–3604
57. Guo J, Long J, Ding D, Wang Q, Shan Y, Umar A, Zhang X, Weeks BL, Wei S, Guo Z-H (2016) Significantly enhanced mechanical and electrical properties of epoxy nanocomposites reinforced with low loading of polyaniline nanoparticles. RSC Adv 6:21187–21192
58. Zhu J, Wei S, Ryu J, Budhathoki M, Liang G, Guo Z-H (2010) In situ stabilized carbon nanofiber (CNF) reinforced epoxy nanocomposites. J Mater Chem 20:4937–4948
59. Chen Z, Mu D, Liu T, He Z, Zhang Y, Yang H, Ouyang J (2021) PANI/$BaFe_{12}O_{19}$@Halloysite ternary composites as novel microwave absorbent. J Colloid Interface Sci 582:137–148
60. Liu Y, Li Y, Jiang K, Tong G, Lv T, Wu W (2016) Controllable synthesis of elliptical Fe_3O_4@C and Fe_3O_4/Fe@C nanorings for plasmon resonance-enhanced microwave absorption. J Mater Chem C 4:7316–7323
61. Li Y, Sun N, Liu J, Hao X, Du J, Yang H, Li X, Cao M (2018) Multifunctional $BiFeO_3$ composites: absorption attenuation dominated effective electromagnetic interference shielding and electromagnetic absorption induced by multiple dielectric and magnetic relaxations. Compos Sci Technol 159:240–250
62. Lu X, Zhu D, Li X, Li M, Chen Q, Qing Y (2021) Gelatin-derived N-doped hybrid carbon nanospheres with an adjustable porous structure for enhanced electromagnetic wave absorption. Adv Compos Hybrid Mater 4:946–956
63. Ding L, Zhang A, Lu H, Zhang Y, Zheng Y (2015) Enhanced microwave absorbing properties of PVP@multi-walled carbon nanotubes/graphene three-dimensional hybrids. RSC Adv 5:83953–83959